Boron Polylactide Nanoparticles Exhibiting Fluorescence and Phosphorescence in Aqueous Medium

ARTICLE *in* ACS NANO · JUNE 2008

Impact Factor: 12.88 · DOI: 10.1021/nn7003525 · Source: PubMed

Published in final edited form as:
ACS Nano. 2008 June ; 2(6): 1252–1258. doi:10.1021/nn7003525.

Boron Polylactide Nanoparticles Exhibiting Fluorescence and Phosphorescence in Aqueous Medium

Anne Pfister[†], **Guoqing Zhang**[†], **Jessica Zareno**[‡], **Alan F. Horwitz**[‡], and **Cassandra L. Fraser**[†,*]

†*Department of Chemistry, University of Virginia, McCormick Road, Charlottesville, Virginia 22904*

‡*Department of Cell Biology, School of Medicine, University of Virginia, Charlottesville, Virginia 22908*

Abstract

Difluoroboron dibenzoylmethane-polylactide, BF_2dbmPLA, a biocompatible polymerluminophore conjugate was fabricated as nanoparticles. Spherical particles <100 nm in size were generated *via* nanoprecipitation. Intense blue fluorescence, two-photon absorption, and long-lived room temperature phosphorescence (RTP) are retained in aqueous suspension. The nanoparticles were internalized by cells and visualized by fluorescence microscopy. Luminescent boron biomaterials show potential for imaging and sensing.

Keywords

boron dye; fluorescence; phosphorescence; poly(lactic acid) (PLA); nanoparticles

Difluoroboron-based dyes, such as BODIPY[1] and β-diketonate derivatives,[2] exhibit large extinction coefficients, high emission quantum yields, large two-photon absorption cross-sections, and in some cases, sensitivity to the surrounding medium.[3] These exceptional optical properties make them useful as imaging agents,[4] photosensitizers,[5] and sensors.[6] Often dyes are combined with material substrates to modulate properties, enhance stability, and reduce toxicity. Dye leaching with associated toxicity and ambiguity in imaging and sensing schemes can be minimized with dye-polymer conjugates versus blends.[7] For example, active agents such as Ru(II) complexes[8,9] or metalloporphyrins[10] are embedded in polymer matrices that act as protective shells and allow their use in biological contexts with increased stability and improved delivery[11,12] by passive[13,14] or active targeting.[15] Many multifunctional imaging and sensing agents combine controlled material synthesis with nanofabrication.[16,17] Nanoparticles based on luminescent dye conjugates and quantum dots[18] are used to label intracellular structures and pathways in fundamental studies as well as for therapeutic and diagnostic purposes.[19,20] Both fluorescence (singlet) and phosphorescence (triplet) emitters are widely used. Phosphorescence, in particular, is susceptible to oxygen quenching *via* triplet energy transfer, serving as the basis for oxygen sensing.[21-23] Good oxygen permeability and fast response time are important factors. Photodynamic therapy, on the other hand, utilizes photosensitizers in combination with oxygen or other quenchers to generate reactive species for selective tissue treatment.[24-26]

Previously we reported that when boron difluoride dibenzoylmethane (BF_2dbm) is combined with poly(lactic acid) (PLA), a biocompatible polymer,[27] the intense blue fluorescence is retained and new properties emerge, namely temperature-sensitive delayed fluorescence and

*Address correspondence to fraser@virginia.edu.

green oxygen-sensitive room-temperature phosphorescence (RTP).[28] (We are unaware of similar multiemissive behavior for a single component BODIPY system at room or elevated temperatures.) The light emitting biomaterial, BF_2dbmPLA, is readily processable as films, fibers, and particles. As a first step in exploring the potential of this class of materials for biological imaging, sensing and photodynamic therapies, we fabricate BF_2dbmPLA as nanoparticles (<100 nm), verify that the unique emission properties persist in an aqueous environment, and demonstrate that cellular uptake of nanoparticles occurs without acute toxicity.

RESULTS AND DISCUSSION

Difluoroboron dibenzoylmethane polylactide, BF_2dbmPLA (Figure 1), was synthesized by ring opening polymerization of lactide using a hydroxyl-functionalized BF_2dbm initiator and tin catalyst as previously described.[28] Nanoparticles were produced by the solvent displacement method (*i.e*., nanoprecipitation)[29,30] in which the polymer is dissolved in a solvent miscible with water (*e.g*., DMF) (oil phase), which is added to water, leading to the formation of droplets. Solvent diffusion results in a supersaturated oil phase, causing the formation of smaller droplets and a meta-stable emulsion.[31] This method of fabrication was selected because nanoparticles of small size are typically obtained, particularly when DMF is used as the organic phase.[25,32] In addition, the nanoprecipitation method avoids sonication that can damage the dye by shear forces and surfactants that can compete with the ligands, as we have observed previously for metal complexes.[33] After fabrication, the morphology, size, chemical integrity, and optical properties of the nanoparticles were investigated. Preliminary cellular uptake studies were also performed.

Particle morphology and size were assessed by transmission electron microscopy (TEM) and dynamic light scattering (DLS). Spherical and fairly homogeneous particles were observed by TEM (Figure 2). Dynamic light scattering measurements indicated that suspended particles were 96 ± 8 nm in size with a polydispersity, Pd = 0.21 ± 0.03 (average of four preparations) and that the fabrication method showed good reproducibility. Because filtration can be important for biological studies, nanoparticle size was also assessed after passage through 0.2 μm nylon syringe filters. The size decreased (89 ± 8 nm) and the polydispersity increased slightly (Pd = 0.23 ± 0.07) under these conditions. A significant decrease in the particle size (68 nm, Pd = 0.23) was observed when an automatic syringe pump was used for the controlled addition of a larger volume of the polymer solution (20 *vs* 5 mL) to the water (200 *vs* 50 mL). These parameters are not usually cited in the literature as determinant of particle sizes, whereas the polymer concentration in the organic solvent and the volume ratio of the polymer solution to the water are and were kept constant in all the preparations.[30,34]

The chemical integrity of BF_2dbmPLA after nanofabrication was assessed for a freeze-dried nanoparticle sample subsequently dissolved in appropriate solvents for gel permeation chromatography (GPC) and ^{1}H NMR, UV-vis and fluorescence spectroscopies. GPC traces for the starting material (M_n = 10400, PDI = 1.18) and nanoparticle sample (M_n = 10400, PDI = 1.12) were similar. Polymer stability was further confirmed by ^{1}H NMR spectroscopy, which also verified the efficient removal of DMF by dialysis. The UV-vis (Figure 3) and fluorescence (Figure 5) spectra for BF_2dbmPLA in CH_2Cl_2 before and after fabrication are also similar (UV-vis: λ_{max} = 396 nm, $\varepsilon = 3.65 \times 10^4$ M^{-1} cm^{-1} (before), $\varepsilon = 3.54 \times 10^4$ M^{-1} cm^{-1} (after); fluorescence: λ_{em} = 426 nm (before), λ_{em} = 426 nm (after)). Thus, the covalently attached boron fluorophore is not damaged during nanoparticle fabrication.

The optical properties of the nanoparticles in aqueous suspension were also investigated. UV-vis spectra for the BF_2dbmPLA particle suspensions are nearly identical to spectra for CH_2Cl_2 polymer solutions except that for the suspension the peak at 383 nm is more

pronounced than the one at 398 nm (Figure 3). The strong blue fluorescence is also observed for nanoparticles in aqueous suspension (λ_{em} = 440 nm) (Figures 4 and 5). Compared to CH_2Cl_2 solutions, a small red shift is observed (Figure 5), which is similar to BF_2dbmPLA solids (films: λ_{em} = 440 nm, powders: λ_{em} = 442 nm). The red-shifted spectrum may be indicative of dye-dye interaction in a single nanoparticle.[35] Thus, the fluorescence properties of the colloidal suspensions and solids are in accord. Though suspensions can present challenges for optical measurements due to scattering, the fluorescence quantum yield for the particles was nonetheless measured and estimated as ϕ_F = 0.55. This value is lower than for BF_2dbmPLA in CH_2Cl_2 (ϕ_F = 0.89)[28] but still higher than commonly used dyes.[36] The fluorescence lifetimes for the nanoparticles in aqueous suspension fit to a double exponential decay: τ_1 = 3.3 ns (96%) and τ_2 = 16.7 ns (4%). Double or multiexponential decay is common for BF_2dbmPLA and other polymer-dye solids and may be attributable to fluorophore interaction or heterogeneous polymer microenvironments. Two-photon absorption, valuable for cell and tissue imaging with increased resolution and reduced damage[37] and well documented for difluoroboron diketonate dyes,[3] is conserved for the BF_2dbmOH initiator. Preliminary results also indicate that BF_2dbmPLA nanoparticles may be visualized using multiphoton microscopy (λ_{ex} = 790 nm).

As previously demonstrated for films,[28] BF_2dbmPLA nanoparticle suspensions also exhibit long-lived room temperature phosphorescence (RTP) and consequently high sensitivity to oxygen quenching, making this system attractive for oxygen sensing applications. This may be contrasted with metal complex luminophores (such as Ru, Ln) that are sensitive to static and dynamic quenching in aqueous environments due to water coordination or O-H vibration.[38,39] The delayed emission spectrum for BF_2dbmPLA nanoparticles is similar to that of the film (RTP, λ_{em} = 509 nm; delayed fluorescence, λ_{em} ~450 nm) (Figure 5). At body temperature (37 °C), the phosphorescence is conserved, an important prerequisite to the use of these nanomaterials in biological contexts. The thermally repopulated delayed fluorescence at ~450 nm[28] is increased slightly at elevated temperature, as expected. Preliminary studies suggest that nanoparticles in aqueous suspension (15 min Ar purge) and BF_2dbmPLA films under vacuum exhibit similar phosphorescence lifetimes (~200 ms). In both cases, data fit to triple exponential decay, and lifetimes decrease with increasing oxygen concentration.[40] Compared to existing oxygen sensing systems (Ru(II)-tris(4,7-diphenyl-1,10-phenanthroline)$^{2+}$, 5.3 μs; Pt(II)octaethylporphine ketone, 0.06-0.09 ms;[36] Pd(II) porphyrin ketone, 0.48 ms[41]), BF_2dbmPLA nanoparticles exhibit longer lifetimes and therefore enhanced sensitivity to oxygen quenching. Because PLA is permeable to oxygen, response times can be fast.[42,43]

PLA nanoparticles are known to degrade over 2 years time because of acid-catalyzed ester hydrolysis. The polymer molecular weight decreases slowly for 5 weeks, then more rapidly thereafter.[44,45] To assess the shelf life of boron nanoparticles in aqueous suspension, their stability was monitored over time using GPC, ^{1}H NMR, UV-vis, and fluorescence spectroscopies, and DLS. After 1, 5, and 11 weeks, aliquots were removed and freeze-dried. GPC analysis shows that the molecular weight decreases and the PDI broadens very slightly over time (after preparation, M_n = 10400, PDI = 1.12; 1 week, M_n = 9600, PDI = 1.20; 5 weeks, M_n = 8,700, PDI = 1.22; 11 weeks, M_n =7500, PDI = 1.37). After 11 weeks, the NMR spectrum shows a resonance at 6.8 ppm that is characteristic of the ArC(O)C***H***=C(OH)Ar' proton in the free dbmPLA macroligand, suggesting hydrolysis of "BF_2" from the dbm binding site for a fraction of the sample. However, the associated dbmPLA ArC(O)CH=C(O***H***)Ar' enol proton peak at 16.98 ppm is not evident in BF_2dbmPLA particle samples after 11 weeks; it was only observed in NMR spectra for samples analyzed after 5 months. A decrease in the UV-vis extinction coefficient, ε ($M^{-1}cm^{-1}$) at 396 nm over time is also consistent with degradation of the boron center (1 week: 3.40×10^4; 5 weeks: 2.78×10^4; 11 weeks: 1.94×10^4). Though the absolute intensity of the fluorescence emission necessarily changes with dye degradation, the emission maximum for boron nanoparticles does not vary over time when samples are analyzed

in aqueous suspension or in CH_2Cl_2 solution after freeze-drying. Hydrolysis of BF_2dbmPLA leads to a nonemissive dbmPLA degradation product, with little effect on nanoparticle emission spectra. Even after 8 months, the blue fluorescence is intense and room temperature phosphorescence is still evident for nanoparticle aqueous suspensions. As previously described,[44] the nanoparticle size shows no significant change after 11 weeks (after preparation, 68 nm, Pd = 0.23; 11 weeks, 67 nm, Pd = 0.18).

Given the unique optical properties and good stability exhibited in aqueous suspension over time, further studies exploring the potential of BF_2dbmPLA nanoparticles and related derivatives for biological imaging, sensing, and photodynamic therapies are merited. Cellular uptake and evidence for the lack of acute toxicity are important to some of these applications. As a preliminary test, the cellular uptake of BF_2dbmPLA nanoparticles was verified *in vitro* with Chinese hamster ovary (CHO) cells. The cells were treated with an aqueous suspension of filtered and unfiltered nanoparticles (unfiltered: size = 97 nm, Pd 0.19; filtered/0.2 μm: size = 78 nm, Pd 0.24) at different concentrations. For a concentration as low as 81 μg/mL, nanoparticle internalization was observed by fluorescence microscopy after 1 h, as is typically noted in the literature.[25,46] Fluorescent nanoparticles were evident in the perinuclear region of the cells (Figure 6). After 3 days, fluorescence was still observed and a significant fraction of the cells were still viable. These preliminary observations indicate typical cell uptake behavior and the lack of acute toxicity for boron nanoparticles, verifying that further investigation and materials optimization is merited.

CONCLUSION

In summary, multiemissive BF_2dbmPLA was fabricated as nanoparticles. The preparation of nanoparticles with this single component material results in a well-defined, controllable product. The fabrication is easy and the covalent attachment of the active agent to the polymer matrix avoids more rapid dye hydrolysis and leaching. Optical properties for nanoparticles in aqueous suspension are similar to the solid polymer; intense fluorescence and long-lived room temperature phosphorescence conferring sensitivity to low oxygen levels were observed. Bright fluorescence and phosphorescence are retained for suspensions kept on the shelf for months even with normal degradation of the biodegradable polyester chains and gradual hydrolysis of the luminophores over time. Cell internalization and imaging without acute toxicity, as demonstrated here, combined with the unusually long-lived phosphorescence still present at 37 °C, raise the possibility of optical sensing in anaerobic environments or in hypoxia model systems. Future work will focus on the effect of polymer molecular weight on emission properties,[35] oxygen sensitivity,[40] and toxicity of these multiemissive particles, along with further optimization and testing of these materials for biological applications.

METHODS

Materials and Instrumentation

All chemicals were obtained from Aldrich. Syringe filters (13 mm, disposable filter device, nylon filter membrane) were obtained from Whatman. ^{1}H NMR (300 MHz) spectra were recorded on a UnityInova 300/51 instrument and referenced to the signal for residual protio chloroform at 7.26 ppm. Molecular weights were determined by GPC (THF, 20 °C, 1.0 mL/min) *versus* polystyrene standards on a Hewlett-Packard instrument (series 1100 HPLC) equipped with Polymer Laboratories 5 μm mixed-C columns and connected to UV-vis and RI (Viscotek LR 40) detectors. Data were processed with the OmniSEC software (version 4.2, Viscotek Corp). A correction factor of 0.58 was applied to all data, as previously described.[47] UV-vis spectra were recorded on a Hewlett-Packard 8453 diode-array spectrophotometer. Fluorescence emission spectra of optically dilute samples (abs < 0.1) were recorded on a

FluoroLog fluorometer (Jobin Yvon-Horiba). Photographs in Figure 4 were taken in the dark using a Canon PowerShot SD600 Digital Elph camera with the automatic setting (no flash).

Nanoparticle Preparation

BF_2dbmPLA (200 mg, M_n = 10400) dissolved in DMF (20 mL) was added dropwise to H_2O (200 mL) using an automatic syringe pump. The water was stirred during the addition and the resulting homogeneous suspension was stirred for an additional 30 min. The suspension was then dialyzed in dialysis tubing (Spectra/Por, 12-14 kDa MWCO, Fisher Scientific) under slow stirring against distilled water following the procedure described in Ataman-Onal et al. for complete DMF removal.[48] The suspension was analyzed as is or freeze-dried for further characterization.

Nanoparticle Size Determination

Nanoparticle sizes were determined by dynamic light scattering (90° angle) on a Photocor Complex (Photocor Instruments Inc., MD) equipped with a He-Ne laser (Coherent, CA, model 31-2082, 632.8 nm, 10 mW). Size and polydispersity analysis were performed using DynaLS software (Alango, Israel). The suspension was analyzed as such or diluted (0.5 mL) with Millipore water (9.5 mL). No significant difference of the size and polydispersity was observed in the diluted and undiluted samples although in some measurements larger size species appeared in the samples that were not diluted due to multiscattering.

Transmission Electron Microscopy (TEM)

Drops of the diluted nanoparticle suspension (20 μL/10 mL deionized water) were deposited directly on carbon-coated electron microscope grids and were allowed to dry. Transmission electron microscopy was performed with a JEOL 200CX, tungsten filament, operated at 200 kV using low dose conditions required by the beam sensitivity of the material. Brightfield images were taken using a CCD camera (AMT).

Fluorescence Lifetimes

Time-resolved fluorescence measurements were performed by exciting the nanoparticle suspension under air with 160 fs pulses at 390 nm, the doubled output of a Coherent RegA Ti:Sapphire amplifier operating at 250 kHz. The resulting fluorescence was spectrally resolved with a Chromex 250is Imaging Spectrograph and temporally resolved with a Hamamatsu C4770 Streak Scope. Data were processed using Hamamatsu, Matlab, and Origin software. Emission data were collected twice for each sample to ensure reproducibility. Reported lifetimes represent an average of two runs, fitted for the entire emission curves.

Quantum Yields

The fluorescence quantum yield, ϕ_F, for the nanoparticle aqueous suspension under air was calculated versus anthracene in EtOH as a standard, as previously described[49] using the following values: ϕ_F anthracene = 0.27,[50] n_D^{20} EtOH = 1.36, n_D^{20} H_2O = 1.333. The optically dilute nanoparticle suspension and the EtOH solution of the anthracene standard were prepared in 1 cm path length quartz cuvettes, and absorbances (A < 0.1) were recorded using a Hewlett-Packard 8453 UV/vis spectrometer. Steady state emission spectra were obtained from a custom-built Photon Technology Instruments fluorimeter installed with a Hamamatsu R928 photomultiplier tube and a 150 W Xe excitation lamp. PTI Felix 32 software was used to process the data (λ_{ex} = 355 nm; emission integration range: 362-700 nm). Emission data were collected three times and averaged. The average spectra were used in the quantum yield calculation.

Multiphoton Microscopy

BF_2dbmPLA nanoparticles may be visualized upon excitation with a femtosecond mode locked Ti:sapphire laser (λ_{ex} = 790 nm) (Coherent, Inc.; pulse width, < 150 fs; repetition rate, 76 MHz; X-wave optics; pumping laser, Verdi, 532 nm, 5 W) using a Nikon PCM2000 laser scanning confocal coupled to a TE-200 epifluorescence microscope, using Simple PCI software.

Phosphorescence Spectra

The aqueous nanoparticle suspension (~5 mL) in a vial was capped with a rubber septum and purged with N_2 for ~15 min. Emission spectra were recorded with an OceanOptics USB2000 fiber optic spectrometer using a hand-held UV lamp (λ_{ex} = 365 nm; long wavelength setting). For the delayed emission at 37 °C, the purged sample vial was placed in a temperature controlled Pyrex water bath, the temperature was allowed to equilibrate for ~10 min, and then the spectrum was recorded.

Phosphorescence Lifetimes

Measurements were performed using instrumentation and methods previously described for BF_2dbmPLA films[28] with the following exceptions. An aqueous nanoparticle suspension (~2 mL) was placed in a quartz cuvette sealed with a screw cap containing a septum (Hellma). The suspension was sparged with argon containing variable amounts of oxygen (~0 to 1%) for 15 min, before lifetime data were recorded.

Cell Culture

Chinese hamster ovary cells (CHO-K1; P10) were seeded with a complete growth media Dulbecco's Modified Essential Medium (DMEM) (1X) liquid (low glucose) (Gibco) containing 1,000 mg/L D-glucose, L-glutamine, pyridoxine HCl, and 110 mg/L sodium pyruvate and supplemented with 10% fetal bovine serum, 1 mM nonessential amino acids, and 1 mM penicillin-streptomycin. The cells were trypsinized and plated on fibronectin-treated (2 μg) glass-bottom 35 mm tissue culture dishes and allowed to spread for 2 h. The nanoparticle suspension (1, 10, 100, and 500 μL) was diluted in complete media (1 mL) and plated on the cells for 1 h incubation at 37 °C and 8.5% CO_2. After incubation, the cells were rinsed twice with 1X PBS and replaced with CCM1 media for imaging. Nanoparticle cellular uptake was observed with a Nikon IX 300 brightfield and fluorescence microscope. The images were obtained with a Retiga camera with the Metamorph Imaging Software (DAPI filter/cube (ex 330-380/em 435-485); 1000 ms exposure).

Acknowledgment

We thank the following persons for experimental assistance, use of facilities, and helpful discussions: (UVA) Prof. J. N. Demas (spectra, phosphorescence lifetime), and Prof. D. L. Green and N. Dutta (DLS); (MIT) D. Alcazar (TEM), R. C. Somers (quantum yield), Dr. S. E. Kooi (fluorescence lifetime), Prof. E. L. Thomas, and Prof. D. G. Nocera. This work was supported by the National Science Foundation (Grants BES-0402212, CHE-0350121) (C.L.F.), the National Institutes of Health (Cell Migration Consortium GM64346, GM23244) (A.F.H.), and the Radcliffe Institute for Advanced Study at Harvard University (C.L.F.).

REFERENCES AND NOTES

1. BODIPY = 4,4-difluoro-4-bora-3a,4a-diaza-s-indacene.Loudet A, Burgess K. BODIPY Dyes and Their Derivatives: Syntheses and Spectroscopic Properties. Chem. Rev 2007;107:4891–4832. [PubMed: 17924696]
2. Chow YL, Johansson CI, Zhang Y-H, Gautron R, Yang L, Rassat A, Yang S-Z. Spectroscopic and Electrochemical Properties of 1,3-Diketonatoboron Derivatives. J. Phys. Org. Chem 1996;9:7–16.

3. Cogné-Laage E, Allemand J-F, Ruel O, Baudin J-B, Croquette V, Blanchard-Desce M, Jullien L. Diaroyl(methanato)boron Difluoride Compounds as Medium-Sensitive Two-Photon Fluorescent Probes. Chem. Eur. J 2004;10:1445–1455.
4. Haugland, RP. The Handbook-A Guide to Fluorescent Probes and Labeling Technologies. Vol. 10th ed.. Spence, MTZ., editor. Molecular Probes; Eugene, OR: 2005. Chapter 1, Section 1.4
5. Yogo T, Urano Y, Ishisuka Y, Maniwa F, Nagano T. Highly Efficient and Photostable Photosensitizer Based on BODIPY Chromophore. J. Am. Chem. Soc 2005;127:12162–12163. [PubMed: 16131160]
6. Méallet-Renault R, Hérault A, Vachon J-J, Pansu RB, Amigoni-Gerbier S, Larpent C. Fluorescent Nanoparticles as Selective Cu(II) Sensors. Photochem. Photobiol. Sci 2006;5:300–310. [PubMed: 16520865]
7. Sun H, Scharff-Poulsen AM, Gu H, Almdal K. Synthesis and Characterization of Ratiometric, pH Sensing Nanoparticles with Covalently Attached Fluorescent Dyes. Chem. Mater 2006;18:3381–3384.
8. Carraway ER, Demas JN, DeGraff BA, Bacon JR. Photophysics and Photochemistry of Oxygen Sensors Based on Luminescent Transition-Metal Complexes. Anal. Chem 1991;63:337–342.
9. Guice KB, Caldorera ME, McShane MJ. Nanoscale Internally Referenced Oxygen Sensors Produced From Self-Assembled Nanofilms on Fluorescent Nanoparticles. J. Biomed. Opt 2005;10:64031-1–64031-10.
10. Briñas RP, Troxler T, Hochstrasser RM, Vinogradov SA. Phosphorescent Oxygen Sensor with Dendritic Protection and Two-Photon Absorbing Antenna. J. Am. Chem. Soc 2005;127:11851–11862. [PubMed: 16104764]
11. Koo YE, Cao Y, Kopelman R, Koo SM, Brasuel M, Philbert MA. Real-Time Measurements of Dissolved Oxygen Inside Live Cells by Organically Modified Silicate Fluorescent Nanosensors. Anal. Chem 2004;76:2498–2505. [PubMed: 15117189]
12. Zhu H, McShane MJ. Loading of Hydrophobic Materials into Polymer Particles: Implications for Fluorescent Nanosensors and Drug Delivery. J. Am. Chem. Soc 2005;127:13448–13449. [PubMed: 16190679]
13. Maeda H, Wu J, Sawa T, Matsumura Y, Hori K. Tumor Vascular Permeability and the EPR Effect in Macromolecular Therapeutics: A Review. J. Controlled Release 2000;65:271–284.
14. Brigger I, Dubernet C, Couvreur P. Nanoparticles in Cancer Therapy and Diagnosis. Adv. Drug Delivery Rev 2002;54:631–651.
15. LaVan DA, McGuire T, Langer R. Small-Scale Systems for in Vivo Drug Delivery. Nat. Biotechnol 2003;21:1184–1191. [PubMed: 14520404]
16. Whitesides GM. Nanoscience, Nanotechnology, and Chemistry. Small 2005;1:172–179. [PubMed: 17193427]
17. Farokhzad OC, Langer R. Nanomedicine: Developing Smarter Therapeutic and Diagnostic Modalities. Adv. Drug Delivery Rev 2006;58:1456–1459.
18. Medintz IL, Uyeda HT, Goldman ER, Mattoussi H. Quantum Dot Bioconjugates for Imaging, Labelling and Sensing. Nat. Mater 2005;4:435–446. [PubMed: 15928695]
19. Torchilin VP. Fluorescence Microscopy to Follow the Targeting of Liposomes and Micelles to Cells and Their Intracellular Fate. Adv. Drug Delivery Rev 2005;57:95–109.
20. Licha K, Olbrich C. Optical Imaging in Drug Discovery and Diagnostic Applications. Adv. Drug Delivery Rev 2005;57:1087–1108.
21. Vanderkooi JM, Maniara G, Green TJ, Wilson DF. An Optical Method for Measurement of Dioxygen Concentration Based Upon Quenching of Phosphorescence. J. Biol. Chem 1987;262:5476–5482. [PubMed: 3571219]
22. Sánchez-Barragán I, Costa-Fernández JM, Valledor M, Campo JC, Sanz-Medel A. Room-Temperature Phosphorescence (RTP) for Optical Sensing. Trend. Anal. Chem 2006;25:958–967.
23. Cochran DM, Fukumura D, Ancukiewicz M, Carmeliet P, Jain RK. Evolution of Oxygen and Glucose Concentration Profiles in a Tissue-Mimetic Culture System of Embryonic Stem Cells. Ann. Biomed. Eng 2006;34:1247–1258. [PubMed: 16832606]
24. Gao D, Agayan RR, Xu H, Philbert MA, Kopelman R. Nanoparticles for Two-Photon Photodynamic Therapy in Living Cells. Nano Lett 2006;6:2383–2386. [PubMed: 17090062]

25. McCarthy JR, Perez JM, Bruckner C. Weissleder, R. Polymeric Nanoparticle Preparation that Eradicates Tumors. Nano Lett 2005;5:2552–2556. [PubMed: 16351214]
26. Konan YN, Chevallier J, Gurny R, Allémann E. Encapsulation of p-THPP into Nanoparticles: Cellular Uptake, Subcellular Localization and Effect of Serum on Photodynamic Activity. Photochem. Photobiol 2003;77:638–644. [PubMed: 12870850]
27. Dechy-Cabaret O, Martin-Vaca B, Bourissou D. Controlled Ring-Opening Polymerization of Lactide and Glycolide. Chem. Rev 2004;104:6147–6176. [PubMed: 15584698]
28. Zhang G, Chen J, Payne SJ, Kooi SE, Demas JN, Fraser CL. Difluoroboron Dibenzoylmethane Polylactide Exhibiting Room Temperature Phosphorescence. J. Am. Chem. Soc 2007;129:8942–8943. [PubMed: 17608480]
29. Fessi H, Puisieux F, Devissaguet J. Ph. Ammoury N, Benita S. Nanocapsule Formation by Interfacial Polymer Deposition Following Solvent Displacement. Int. J. Pharm 1989;55:R1–R4.
30. Avgoustakis K. Pegylated Poly(lactide) and Poly(lactide-co-glycolide) Nanoparticles: Preparation, Properties and Possible Applications in Drug Delivery. Curr. Drug Delivery 2004;1:321–333.
31. Ganachaud F, Katz JL. Nanoparticles and Nanopcapsules Created Using the Ouzo Effect: Spontaneous Emulsification as an Alternative to Ultrasonic and High-Shear Devices. Chem. Phys. Chem 2005;6:209–216. [PubMed: 15751338]
32. Cheng J, Teply BA, Sherifi I, Sung J, Luther G, Gu FX, Levy-Nisenbaum E, Radovic-Moreno AF, Langer R, Farokhzad OC. Formulation of Functionalized PLGA-PEG Nanoparticles for *in Vivo* Targeted Drug Delivery. Biomaterials 2007;28:869–876. [PubMed: 17055572]
33. Pfister A, Chen J, Chen YJ, Fraser CL. Iron Tris(dibenzoylmethane-polylactide) Nanoparticles. Polym. Mater. Sci. Eng 2007;96:923.
34. Bilati U, Allémann E, Doelker E. Development of a Nanoprecipitation Method Intended for the Entrapment of Hydrophilic Drugs into Nanoparticles. Eur. J. Pharm. Sci 2005;24:67–75. [PubMed: 15626579]
35. Zhang G, Kooi SE, Demas JN, Fraser CL. Emission Color Tuning with Polymer Molecular Weight for Difluoroboron Dibenzoylmethane-Polylactide. Adv. Mater. 2008in press
36. As examples, for Ru(II)-tris(4,7-diphenyl-1,10-phenanthroline) $^{2+}$, f_F = 0.3; for Pt(II) octaethylporphine ketone, f_F = 0.1-0.5; see:Cao Y, Koo Y-EL, Kopelman R. Poly(decyl methacrylate)-Based Fluorescent PEBBLE Swarm Nanosensors for Measuring Dissolved Oxygen in Biosamples. Analyst 2004;129:745–750. [PubMed: 15284919]
37. So PT, Dong CY, Masters BR, Berland KM. Two-Photon Excitation Fluorescence Microscopy. Annu. Rev. Biomed. Eng 2000;2:399–429. [PubMed: 11701518]
38. Delgadillo A, Arias M, Leiva AM, Loeb B, Meyer GJ. Interfacial Charge-Transfer Switch: Ruthenium-dppz Compounds Anchored to Nanocrystalline TiO_2. Inorg. Chem 2006;45:5721–5723. [PubMed: 16841970]
39. Huignard A, Buissette V, Franville A-C, Gacoin T, Boilot J-P. Emission Processes in YVO_4:Eu Nanoparticles. J. Phys. Chem. B 2003;107:6754–6759.
40. Technical challenges associated with simultaneous control of oxygen concentration and temperature for boron nanoparticles preclude detailed quantitative calibration of oxygen sensitivity with the present setup. Alternative instrumentation for sensitive oxygen calibration measurements requires modification for long phosphorescence lifetimes. (For example, see:Rozhkov V, Wilson DF, Vinogradov S. Phosphorescent Pd Porphyrin-Dendrimers: Tuning Core Accessibility by Varying the Hydrophobicity of the Dendrimer Matrix. Macromolecules 2002;35:1991–1993.Supporting Information.) Oxygen calibration of BF_2dbmPLA nanoparticles requiring the development of new instrumentation will serve as the subject of future reports.
41. Papkovsky DB, Ponomarev GV, Trettnak W, O'Leary P. Phosphorescent Complexes of Porphyrin Ketones: Optical Properties and Application to Oxygen Sensing. Anal. Chem 1995;67:4112–4117.
42. Auras R, Harte B, Selke S. Effect of Water on the Oxygen Barrier Properties of Poly(ethylene terephthalate) and Polylactide Films. J. Appl. Polym. Sci 2004;92:1790–1803.
43. Bao L, Dorgan JR, Knauss D, Hait S, Oliveira NS, Maruccho IM. Gas Permeation Properties of Poly (lactic acid) Revisited. J. Membr. Sci 2006;285:166–172.

44. Zweers MLT, Engbers GHM, Grijpma DW, Feijen J. *In Vitro* Degradation of Nanoparticles Prepared from Polymers Based on d,l-Lactide, Glycolide and Poly(ethylene oxide). J. Controlled Release 2004;100:347–356.
45. Alexis F. Factors Affecting the Degradation and Drug-Release Mechanism of Poly(lactic acid) and Poly[(lactic acid)-*co*-(glycolic acid)]. Polym. Int 2005;54:36–46.
46. Panyama J, Sahoo SK, Prabha S, Bargar T, Labhasetwar V. Fluorescence and Electron Microscopy Probes for Cellular and Tissue Uptake of Poly(d,l-lactide-*co*-glycolide) Nanoparticles. Int. J. Pharm 2003;262:1–11. [PubMed: 12927382]
47. Gorczynski JL, Chen J, Fraser CL. Iron Tris(dibenzoylmethane)-Centered Polylactide Stars: Multiple Roles for the Metal Complex in Lactide Ring-Opening Polymerization. J. Am. Chem. Soc 2005;127:14956–14957. [PubMed: 16248597]
48. Ataman-Onal Y, Munier S, Ganée A, Terrat C, Durand P-Y, Battail N, Martinon F, Le Grand R, Charles M-H, Delair T, Verrier B. Surfactant-Free Anionic PLA Nanoparticles Coated with HIV-1 p24 Protein Induced Enhanced Cellular and Humoral Immune Responses in Various Animal Models. J. Controlled Release 2006;112:175–185.
49. Demas JN, Crosby GA. Measurement of Photoluminescence Quantum Yields. Review. J. Phys. Chem 1971;75:991–1024.
50. Melhuish WH. Quantum Effeciencies of Fluorescence of Organic Substances: Effect of Solvent and Concentration of the Fluorescent Solute. J. Phys. Chem 1961;65:229–235.

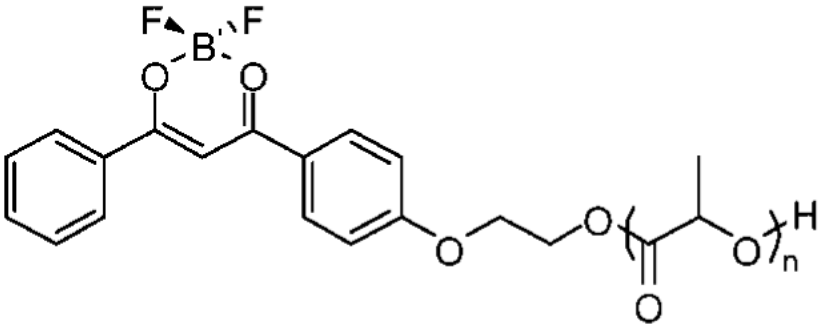

Figure 1.
Chemical structure of BF_2dbmPLA.

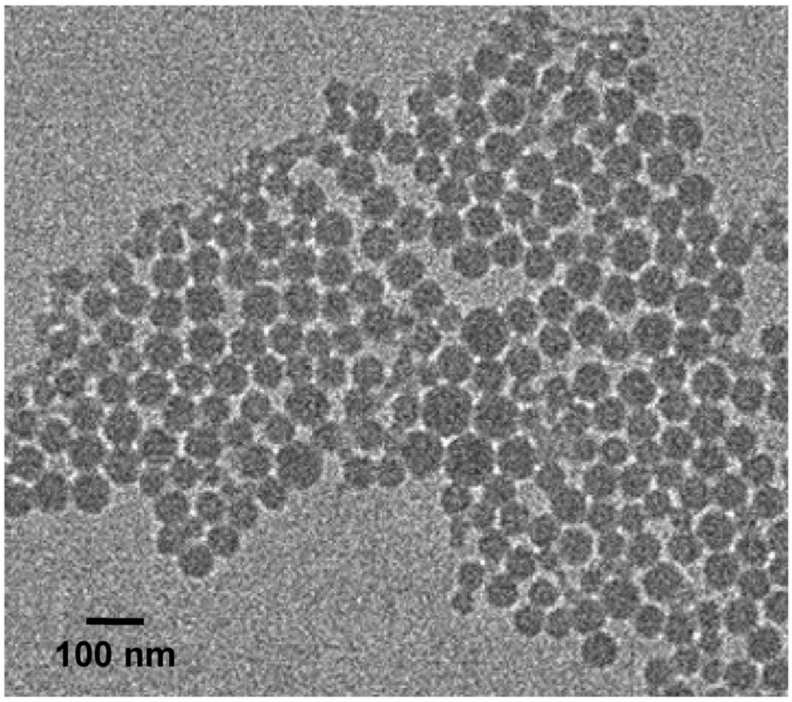

Figure 2.
TEM image of BF_2dbmPLA nanoparticles.

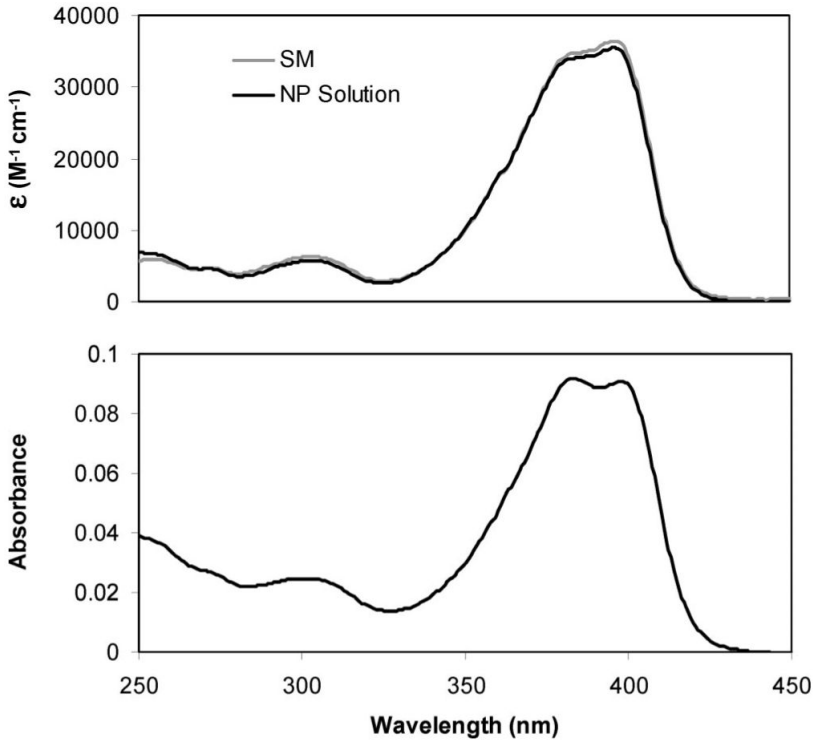

Figure 3.
UV-vis absorption spectra for the BF_2dbmPLA starting material (SM) and freeze-dried nanoparticles (NP) dissolved in CH_2Cl_2 (~2 μM; top) and for the nanoparticles in aqueous suspension (~0.03 mg/mL; bottom).

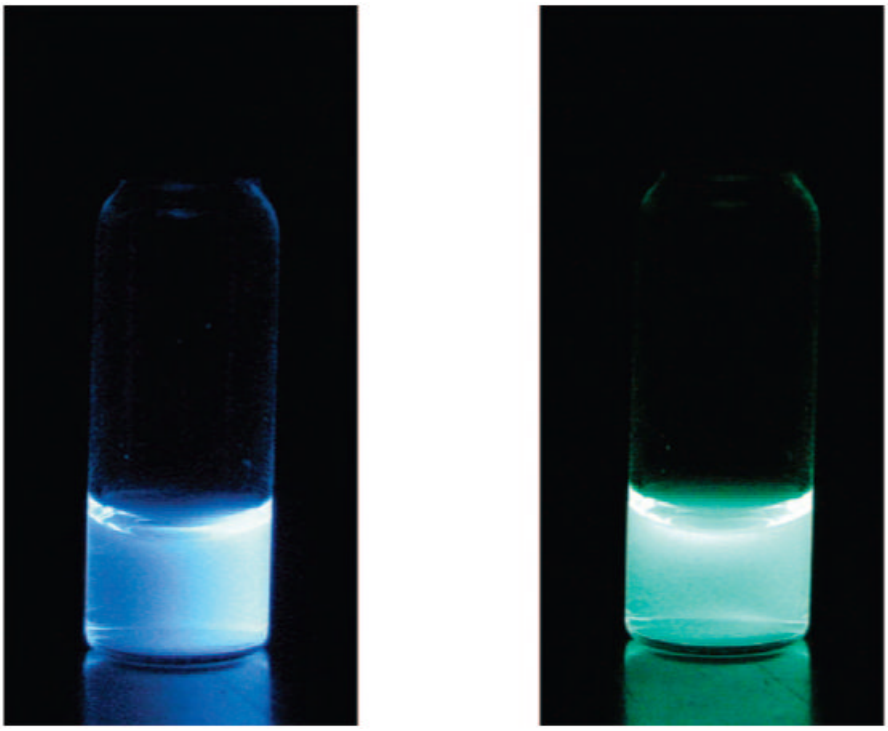

Figure 4.
Images showing fluorescence (left) and phosphorescence (right) of the nanoparticle aqueous suspension. (Fluorescence under air; phosphorescence imaged under a nitrogen atmosphere after the excitation source is turned off. λ_{ex} = 365 nm.)

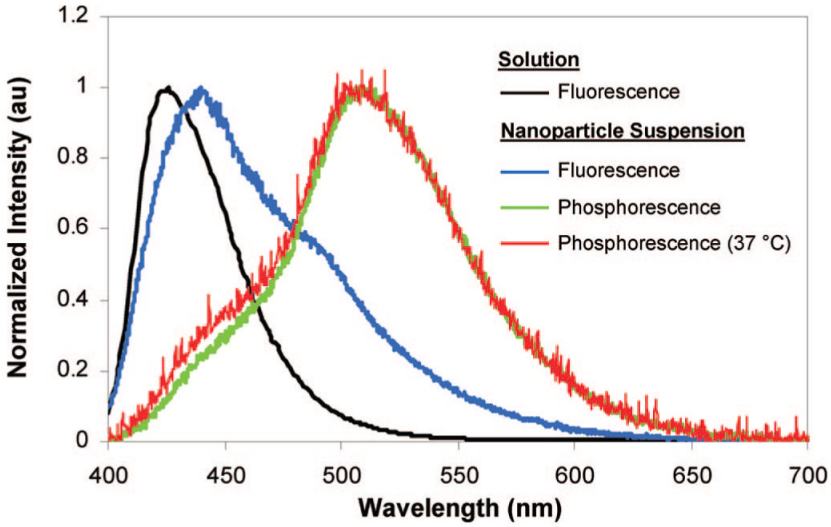

Figure 5.
Normalized emission spectra for BF_2dbmPLA in CH_2Cl_2 solution and as an aqueous nanoparticle suspension (at 22 °C, unless otherwise specified).

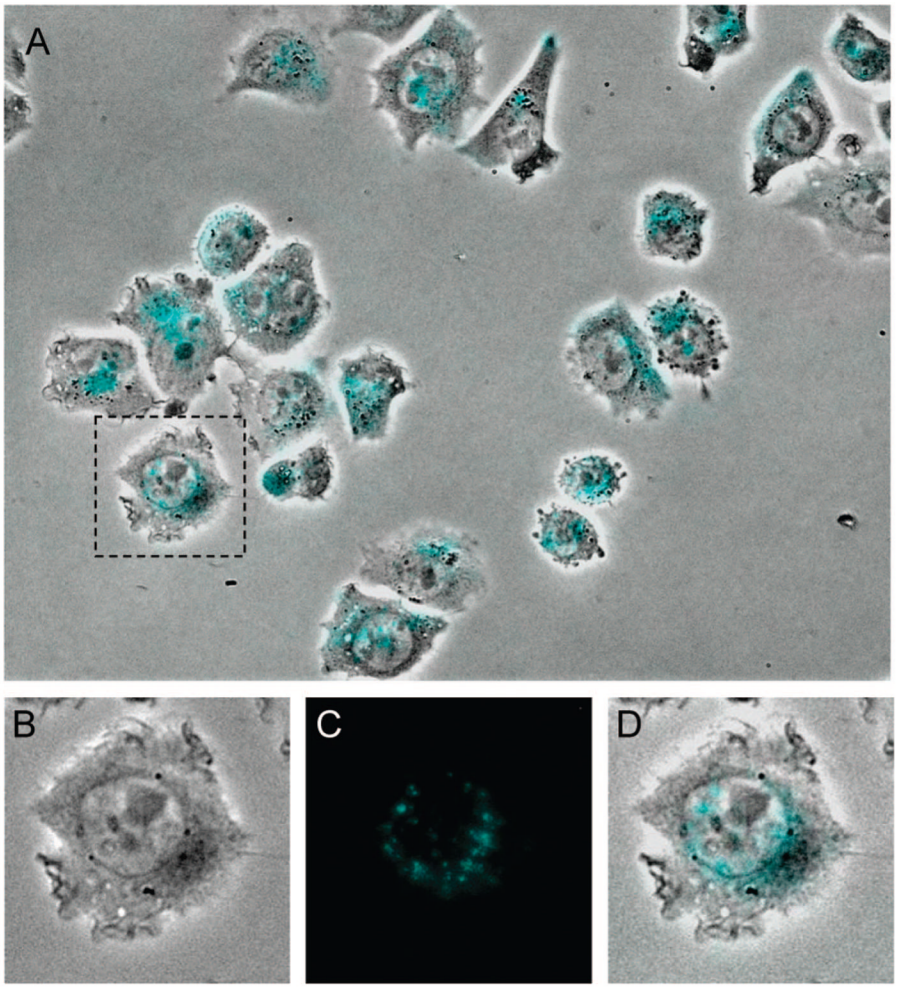

Figure 6.
Fluorescence and bright field microscopy image overlay (A) of CHO cells incubated for one hour with a filtered BF_2dbmPLA nanoparticle suspension (405 μg/mL before filtration) and images of one cell showing the perinuclear localization of the fluorescent nanoparticles (bright field (B), fluorescence (C), and overlay (D) microscopy images; false color image).